

## MECHANICAL STRUCTURE DESIGN AND PERFORMANCE ANALYSIS OF HEAT STORAGE WORKING MEDIUM FOR HEAT INSULATION LAYER

by

**Zhiwei HUANG\* and Yan ZHANG**

Yellow River Conservancy Technical Institute,  
Mechanical Engineering Department, Henan, Kaifeng, China

Original scientific paper  
<https://doi.org/10.2298/TSCI2402271H>

*In order to solve the problems of low temperature inside the greenhouse caused by continuous haze weather or cloudy, rainy, and snowy weather, as well as the large heat dissipation capacity and insufficient cross time heat storage of existing solar greenhouses, by optimizing the design of the external insulation materials and structure of the heat storage water tank and studying the combination of heat storage working fluids, the greenhouse heat storage device has achieved cross time heat storage and segmented slow release heat release. The experiment shows that the combined heat insulation effect of heat insulation coating + aerogel + rubber and plastic insulation cotton is better; its 24-hour heat dissipation is reduced by 0.367 MJ compared to a single insulation material. The heat preservation material of the tank is 80~120 mm, and the cylinder heat storage tank is 6~10 m<sup>3</sup> and 1:1. Which cannot only ensure a low effective heat dissipation rate, but also control engineering. The results show that the composite phase change material can increase the heat storage capacity, optimize the exothermic process, and achieve the gradual release of heat.*

Key words: *greenhouse, heat storage water tank, insulation materials, phase change materials*

### Introduction

Protected agriculture is a modern agricultural mode that uses certain agricultural engineering technical means and necessary facilities and equipment to carry out efficient production of animals and plants under a relatively controllable environment created by human beings. Meanwhile, in other countries around the world, facility agriculture is also known as controlled environmental. Agriculture, which includes two major basic categories: The first is facility breeding, which is fine breeding management under the condition of agricultural engineering. The second is protected horticulture, also known as protected cultivation in China in the past. In artificially controlled agricultural facilities, vegetable crops are finely cultivated and produced by controlling environmental factors such as light, temperature, water, gas, and fertilizer. The facility horticulture industry plays a crucial role in the development of the agricultural industry [1].

Annual production reduces land use, greatly increases crop yield per unit area, and greatly alleviates the problem of insufficient per capita arable land. At present, the widely used facility types in the field of plant production are greenhouses, including traditional solar greenhouses, active thermal storage solar greenhouses, and the introduced Wenluo type glass green-

\* Corresponding author, e-mail: [jhzsc@zjnu.edu.cn](mailto:jhzsc@zjnu.edu.cn)

houses. In recent years, there have been many explorations in the combination of agricultural facilities and new energy applications in the agricultural field. Among the numerous new energy utilization, solar collectors have the best application effect. Water thermal storage devices combined with solar thermal collectors have received more research in the field of agricultural engineering, and have been used more and more as a new energy utilization mode for protected horticulture. However, there are currently some problems with the supporting water thermal storage devices for greenhouse heat collection devices, especially the lack of research on cross time thermal storage devices.

### Literature review

Facility agriculture, as an efficient modern agricultural model, has been widely promoted and rapidly developed in China in recent years. This large-scale and modern agricultural production model has become a trend in China's agricultural development. However, in the northern region, the winter temperature is low, the duration of light and intensity are small, and continuous rainy and snowy weather results in low greenhouse temperature that cannot meet the normal growth requirements of eggplant crops. In recent years, continuous haze weather has exacerbated this phenomenon. Additional greenhouse warming and heat input are necessary conditions to ensure the normal overwintering production of warm crops in the greenhouse. There are many greenhouse warming measures, among which furnace heating, boiler heating and other methods not only need to consume a large amount of fossil fuels, but also cause environmental pollution. Water thermal storage devices combined with solar thermal collectors have been more studied in the field of agricultural engineering, and have been increasingly used as a new energy utilization method for facility gardening. At present, there are many application forms of water cycle heat collection devices in greenhouse facilities, but there is little research on water body heat storage devices that are matched with greenhouse heat collection devices.

Among numerous thermal storage media, water has good heat transfer characteristics and, as a fluid at room temperature, has a small coefficient of thermal expansion and viscosity. Water, as one of the most widely present substances in nature, has a large reserve and low cost of use, making it widely used as a heat storage medium in agricultural facilities. The heat storage tank used simultaneously with the heat collection device in the steel pipe roof truss heat collection and release system is constructed into an external structure using clay bricks. The inner wall of the water tank as the heat storage medium is coated with waterproof paint, and the outer wall of the water tank is bonded with 10 cm thick foam polystyrene board for insulation. In the heat storage device used at the same time with the heat collection device in the water curtain heat storage system, the heat storage device is welded by polyester hard plate, and its external thermal insulation device is polystyrene foam plate with a thickness of 10 cm, which can play a good role in short-term heat storage. The heat storage device linked to the heat collection device in the hollow plate water circulation system is built with clay bricks, located underground inside the greenhouse, with a volume of 15 m<sup>3</sup>. On the left and right sides, anti-seepage materials are installed on the inner wall of the device, and 100 mm expanded polystyrene board is installed on the outer side of the device as insulation material. There are many application forms of heat storage devices in agricultural facilities, but there is little research on water heat storage devices that are matched with greenhouse heat collectors. Currently, greenhouse heat storage devices have single insulation materials, simple structural design, and large heat loss. Based on the research achievements of scholars both domestically and internationally, there has been a considerable amount of research on thermal storage systems in greenhouse water bodies. This project has also conducted multiple studies on solar energy collection systems, but there

is relatively little research on thermal storage devices that are compatible with the collection system, especially on the structure, thermal storage capacity, and materials of cross time thermal storage devices.

Nordbeck *et al.* [2] carried out experimental and numerical analysis of a new type of heat storage system with cement base, water saturation, and spiral pipe heat exchanger. Two special, highly controlled dynamic charge and discharge experiments were carried out on a 1 m<sup>3</sup> lab prototype memory cell to characterize the storage system from the perspective of memory rate and capacity [3]. Wang *et al.* [4] started to assess the influence of HTF temperature on the heat storage and mechanical properties of heat-layered containers with solar PCM capsules and binary nitrate molten salt. The cycle process of the storage tank is modeled with fixed parameters. The results indicate that the tank works stably, the charging time is 365.0 minutes, the discharge time is 264.0 minutes. Dong *et al.* [5] put forward a kind of LHTESS based on biomimetic pulsed-layered structure, which can increase the heat transfer rate and storage efficiency of LHTESS. Similar to a conventional homogeneous structure, the size of a porous heat storage unit is variable in both axial and radial dimensions. The influence of the inlet velocity on the performance, the temperature distribution, the pressure drop and the liquid fraction of the conventional and biomimetic structures were analysed.

In order to solve the problems of single insulating material, simple structure design and high heat loss in the solar energy collecting system, the properties of different insulating materials were compared and combined, and their relevant physical and thermal properties were analyzed and tested. In order to get the optimal thermal preservation effect and performance, the optimum insulation material is obtained. Using mature PCM to enhance heat storage capacity, and applying different phase change combinations to measure the heat release effect of heat storage device. The structure of the heat storage device is optimized, so as to realize the purpose of cross-time heat storage and sectional heat release.

## **Experimental materials and methods**

### *Experimental materials*

The experiment was conducted in a Wenluo style multi-span research greenhouse at a certain agricultural and forestry university (34° 16' N, 107° 59' E), with a greenhouse compartment length of 6 m, width of 4 m, and ridge height of 5 m. The temperature measurement and control range is -30~70 °C, the accuracy is ±5 °C, and the resolution is 0.1 °C. Relative humidity measurement range: 0-99%, accuracy ±3%, resolution 1%. The temperature data in the experimental device is collected using the AT4524 Amber 24 channel inspection instrument, with a temperature measurement and control range of -200~1300 °C, an accuracy of ±0.2 °C, and a resolution of 0.1 °C [6].

### *Insulation layer material selection and composite material experiment*

The experiment used five cylindrical polyethylene water tanks with consistent specifications, with a diameter of 580 ±5 mm, a height of 900 ±5 mm, a thickness of 10 mm, and a volume of 230 L. Under actual greenhouse operating conditions, heat insulation materials with different treatments are added to the outer wall of the water tank, and the water temperature of the heat storage tank is heated to 60 °C, followed by actual heat release testing. The 22 kinds of thermal insulation materials including polystyrene board, extruded board, vacuum board, EPS insulation board, aerogel, rubber wool and composite PCM were collected. Due to the different processing technologies of thermal insulation materials, it is difficult to guarantee the specifications and quality of the materials. The thermal conductivity of the insulated layer was measured

by FDTCB thermal conductivity tester to ensure the thermal conductivity of the insulated layer. To test the relation between the thickness of heat preservation material and the heat dissipation, 10 mm, 30 mm, 50 mm, 80 mm, 100 mm, and 180 mm of rubber plastic heat-preserving cotton were added into the tank. In order to enhance the insulation effect of insulation materials per unit thickness, different insulation materials were used, with materials with high thermal resistance inside and materials with low thermal resistance outside. At the same time, referring to the structural strength and composite fit of the materials, seven insulation combinations with a thickness of 50-100 mm were designed, and composite experiments of different materials were conducted. In the heat insulation material combination experiment, fixed frames and locks are used for external reinforcement, and neutral silicone adhesive is used for sealing between the material gaps to ensure a tight fit between the materials and reduce gap heat dissipation. In practice, the temperature measuring point is set in the joint area of every layer, and the temperature measuring point is arranged in the inner part of the tank. An amber temperature recorder is used for real-time temperature measurement, and the PDEKI multi-channel environmental tester is used to collect the greenhouse environmental temperature.

#### Preparation of phase change composite units

The PCM is packaged using PC tubes, which have two sizes: *m*-type hollow PC tubes with a size of 20 mm × 17 mm × 150 mm and *n*-type hollow PC tubes with a size of 12 mm × 10 mm × 330 mm. The thermal conductivity of palmitic acid, myristic acid and lauric acid is only about 0.16 W/mK, and the thermal conductivity is poor. The thermal conductivity of PCM can be significantly increased by using PCM and graphite composite.

Dry the expanded graphite in a 60 °C vacuum drying oven for 16 hours, then take 1 g and place it in a large beaker. Place it in a regular household microwave oven (with an output power of 800 W), and microwave expand for 30 seconds to obtain wormlike expanded graphite. Weigh 16 g each of palmitic acid, myristic acid and lauric acid into a PC tube sealed at one end, add 1g expanded graphite, and then seal the other end of the sealed tube with molten PC to make a composite phase change unit. Heat the composite phase change unit in a water bath to 70 °C and shake well. Shake well every 10 minutes for a total of 5 times, so that all PCM and expanded graphite are evenly mixed and fully adsorbed.

#### Structure and combined lay-out of heat storage water tank

The structure of the phase change heat storage tank is shown in fig. 1. Three 500 mm × 500 mm × 600 mm test areas are built with metal trusses and 50 mm EPS insulation board. In the middle of each test area, the phase change heat storage tank is filled with homogeneous soil with a moisture content of 65%. The upper part of the test area is covered with

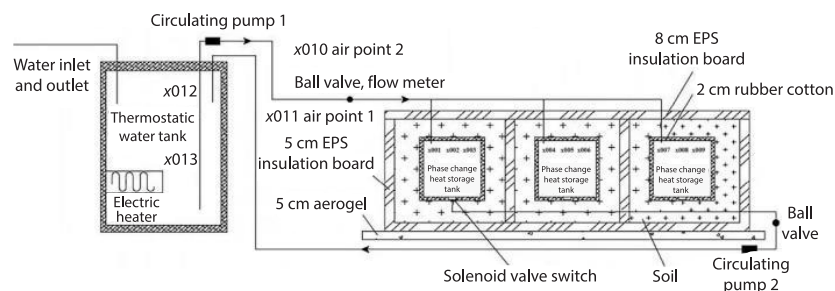


Figure 1. Phase change hot water storage tank structure and main measuring point lay-out

20 mm aerogel and EPS insulation board. The 50 mm aerogel is set between the bottom of the test area and the ground. The experiment used three iron cylindrical barrels with a diameter of 300 mm, a height of 330 mm, a thickness of 1 mm, and a volume of 23 L as the rigid body of the phase change heat storage tank. The 20 mm rubber plastic insulation cotton was installed on the top, bottom, and wall of the tank [7]. The system is equipped with 24 temperature measurement points, with the main temperature measurement points arranged as shown in fig. 1.

The working efficiency of solar collectors in actual greenhouses is significantly affected by the intensity and duration of light, so the supporting heat storage device is set with two working modes: Under Condition 1, the heat collection meets the requirement that water exceeding the volume of the heat storage tank is heated to 65 °C. The hot water cycle is conducted after the injection, and when the measured temperature is in accordance with 65 °C, the cycle is stopped. In the second condition, the heat collecting capacity should not be larger than the capacity of the storage tank, and the heat storage medium should be heated to 65 °C. No hot water cycle shall be performed after injection into the heat storage tank.

Under actual operating conditions, different numbers and types of phase change units are added to the heat storage tank, and heat release tests are conducted after heating cycles. Different phase change combinations were set up in the experiment to test the relationship between the number and types of phase change unit combinations and water tank heat storage. Among them, combination i consists of 30 PA/EGn and 30 LA/EGn units, combination ii consists of 30 MA/EGn and 30 LA/EGn units, and combination iii consists of 30 MA/EGn and 30 PA/EGn units. Combination I consists of PA/EGn, MA/EGn, and LA/EGn unit combinations in a 1:1 configuration, Combination II consists of PA/EGn, MA/EGn, and LA/EGn unit combinations in a 3:2:1 configuration, and Combination III consists of PA/EGn, MA/EGn, and LA/EGn unit combinations in a 1:2:3 configuration.

Among them, the *n*-type phase change units are longer and arranged in a circular *n*-shaped manner. In the mixed phase change experiment, the PA, MA, and LA phase change units are sequentially arranged from the center of the water tank to the barrel wall. The *m*-type phase change unit is relatively short and is arranged in a rectangular *m*-shape. In the mixed phase change experiment, the water tank is composed of PA, MA, and LA phase change units from top to bottom.

#### Water tank heat storage and release model

During the exothermic process process, the heat dissipation capacity of the heat storage tank:

$$Q_s = \int_{\tau_1}^{\tau_2} KA(t_{in,\tau} - t_{out,\tau})d\tau \quad (1)$$

$$\frac{1}{K} = \frac{\delta_t}{\lambda_t} + \frac{\delta'}{\lambda'} \quad (2)$$

When the temperature of the storage tank is below 40 °C, the temperature difference between the greenhouse and the surrounding environment will be very small, resulting in the reduction of heat output. So when the temperature in a greenhouse exceeds 40 °C, we call it effective heat storage. If the temperature in the tank is more than 40 °C, it is called effective heat release:

$$\eta = \frac{KA\tau(t_r - t_e)}{\Delta t_0 C_w \rho_w V_w} \quad (3)$$

where  $t_e$  [°C] is the effective utilization temperature of the greenhouse heat release device.

The energy stored in a regular water tank:

$$Q_w = C_w \rho_w V_w (T_1 - T_2) \quad (4)$$

The energy stored in the phase change heat storage tank:

$$Q_p = C_w \rho_w (V_w - V_p) (T_1 - T_2) + \sum_{i=1}^n \rho_{pi} V_{pi} [C_{li} (T_1 - T_{li}) + \gamma_i + C_{si} (T_{si} - T_2)] \quad (5)$$

## Experimental results and analysis

### Screening and analysis of insulation materials

The FDTCB thermal conductivity of the selected materials was tested in the lab. Table 1 illustrates the actual thermal conductivity of the insulating materials. In accordance with the practical operation, the radiator adopts the insulation material and the rubber plastic insulation sponge, used in heat experiments. Table 2 shows the variation in temperature and the amount of heat produced by the heater. As can be seen from tab. 2, with the increase of the thickness of the insulation layer, the higher the water temperature in the water tank, the smaller the heat dissipation. If the insulation material has a thickness of more than 30 mm, the difference between the actual heat release quantity and the heat release model is less than 5. Thus, it is possible to calculate the heat release of a material's heat storage device using the aforementioned equation [8].

**Table 1. Thermal conductivity of thermal insulation materials**

| Material                     | Thermal conductivity [Wm <sup>-1</sup> K <sup>-1</sup> ] |
|------------------------------|--|
| Polystyrene board            | 0.034  |
| EPS insulation board         | 0.033  |
| ceramic fiber blanket        | 0.035  |
| Rock wool board              | 0.042  |
| Rubber insulation cotton     | 0.041  |
| Polystyrene particle mortar  | 0.144  |
| Aerogel                      | 0.023  |
| Vacuum plate                 | 0.008  |
| Composite insulation coating | 0.035  |

**Table 2. Temperature change and heat dissipation of the heat storage tank for 24 hours**

| Heat insulating material thickness [mm] | Initial temperature [°C] | The 24 hours water tank temperature [°C] | Actual heat dissipation [MJ] | Theoretical heat dissipation [MJ] | Error [%] |
|---|--------------------------|--|------------------------------|-----------------------------------|-----------|
| 10                                      | 60                       | 42.80                                    | 17.59                        | 16.52                             | 6.20      |
| 30                                      | 60                       | 51.90                                    | 7.32                         | 7.51                              | 4.18      |
| 50                                      | 60                       | 55.40                                    | 5.41                         | 5.10                              | 4.10      |
| 80                                      | 60                       | 55.77                                    | 4.09                         | 3.85                              | 3.37      |
| 100                                     | 60                       | 56.24                                    | 3.63                         | 3.52                              | 3.07      |
| 180                                     | 60                       | 56.09                                    | 2.81                         | 2.75                              | 2.15      |

The efficiency of the heat release rate of the heating tank with different insulation thicknesses of 24 hours and 72 hours is shown in fig. 2. The heat dissipation efficiency of the insulation material of the same thickness also increases depending on the length of the heat storage period. At the same time, when the thickness of the insulation material of the heating tank is 0-80 mm, the effective heat dissipation rate of the heating tank is high, which greatly affects the insulation material. If the thickness of the insulating material is greater than 80 mm, the effective heat dissipation rate of the heat storage tank will be small, and the insulating material will not be affected much.

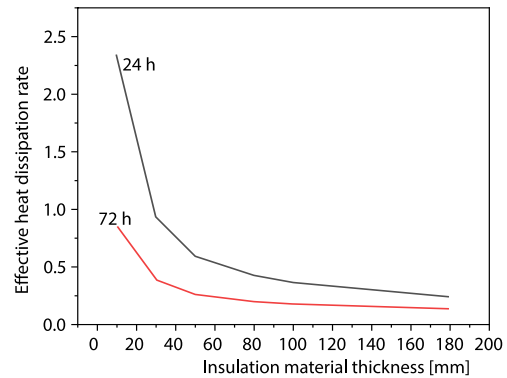


**Figure 2. Effective heat dissipation rate of water tanks with different insulation material thicknesses at different times**

*Performance analysis of insulation composite materials*

Under actual operating conditions, actual heat storage tests were conducted on water tanks with different combinations of insulation materials. The actual 24 hour heat dissipation of each device is shown in tab. 3. From tab, 3, it can be seen that the heat dissipation of the heat storage water tank using Combination 4 is the smallest within 24 hours, which reduces heat dissipation by 0.367 MJ compared to the control group 80 mm rubber plastic insulation cotton water tank.

According to the heat dissipation model calculation, the heat transfer coefficient of different thicknesses of each combination under the same configuration conditions is shown in fig. 3. It can be seen from fig. 3 that under the condition of the same insulation combination thickness, Combination 1-4 has smaller heat transfer coefficient and the best insulation effect [9].

**Table 3. The 24 hours heat dissipation of water tank under different heat insulation material combinations**

| Combination   | Actual heat dissipation capacity of the water tank [MJ] |
|---------------|---|
| Combination 1 | 4.767   |
| Combination 2 | 3.855   |
| Combination 3 | 4.528   |
| Combination 4 | 3.719   |
| Combination 5 | 8.162   |
| Combination 6 | 4.507   |
| Combination 7 | 4.701   |
| Contrast      | 4.076   |

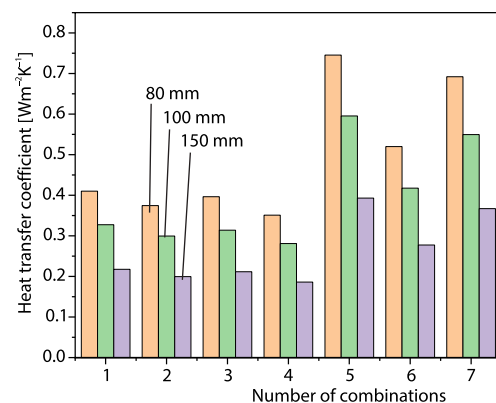


**Figure 3. Heat transfer coefficients of material combinations of different thicknesses**

### *Optimization design of heat storage tank*

When the volume of the heating tank is  $1 \text{ m}^3$ , the heat release of different types of tanks for 24 hours. When the volume of the heating tank is  $1 \text{ m}^3$ , the spherical heat sink has the smallest heat-dissipating surface and the largest heat-dissipating area. The second place is occupied by a cylindrical heat storage tank with a diameter of 1:1. In actual construction, the construction of spherical heat storage tanks is difficult and not often used. Therefore, it is recommended to use a cylindrical heat storage tank with a 1:1 diameter from height to bottom diameter [10, 11]. Insulation materials 4 and 1:1 cooling and cooling characteristics are used in cylindrical containers with a heating diameter of 72 hours. The heat storage tank increases with the volume of the heat storage tank.

### *The influence of thermal storage working fluid on the temperature of thermal storage water tank*

Heat release experiments were conducted on pure water tanks without phase change units and 80 phase change heat storage tanks with MA/EGn units under two operating conditions. There is no obvious effect on the temperature variation of the tank in the experiment. The heating cycle changes the temperature of the heater box in Case 2 during the heating period from 0-500 minutes. In the period of 500~2000 minutes, the temperature of the tank is gradually reduced, and the water temperature is higher than that of the fresh water tank. When the water temperature reaches the phase change region, the phase change region is heated to ensure the water temperature. The exothermic capacity of the tank is increased and the exothermic capacity is reduced by using the phase change radiator.

### **Conclusion**

The thickness of the insulation of the deep water greenhouse in the northern region is 80-120 mm, the use is good, and the cost is relatively low. When the height and bottom diameter ratio is 1:1 and the volume is  $6-10 \text{ m}^3$ , the heating box cannot only increase the heat dissipation efficiency, but also increase the management engineering. The 10 mm thermal insulation layer adopted 20 mm aerogel 50 mm rubber and plastic insulation cotton thermal insulation combination, the heat transfer coefficient is  $0.354 \text{ W/m}^2\text{K}$ . After heating for 24 hours, the heat loss of the device is 0.367 MJ lower than that of 80 mm rubber and plastic insulation sponge, and the thermal insulation effect is the best in the combined measure. However, there are some gaps in the integration of different heat release products, so the technology needs to be improved. The rectangular phase change heat storage tank changes the natural thermal stratification effect of the tank, and the heat storage effect is better than the rectangular phase change. Combined with three types of phase change data, the heating box optimizes the exothermic process, reduces heat output from temperature, and realizes the accuracy of phase heat output.

### **References**

- [1] Zhao, P., *et al.*, Components Design and Performance Analysis of a Novel Compressed Carbon Dioxide Energy Storage System: A Pathway Towards Realizability, *Energy Conversion and Management*, 229 (2021), 1, 113679
- [2] Nordbeck, J., *et al.*, Experimental and Numerical analysis of a Cement Based Thermal Energy Storage System with a Helical Heat Exchanger, *Applied Thermal Engineering*, 185 (2021), 116339
- [3] Wang, Y., Type Door Rigid Frame – Pile Arch System Characteristics and Disaster Prevention Application in Thermodynamics, *Thermal Science*, 23 (2019), 5A, pp. 2749-2755
- [4] Wang, G., *et al.*, Impact Evaluation of Cold Heat Transfer Fluid Temperature on Heat Storage and Mechanical Behaviours of an Energy Storage System Using Phase-Change Material, *International Journal of Thermophysics*, 42 (2021), 5, pp. 1-18



- [5] Dong, Y., *et al.*, Numerical Study on the Thermal Performance Analysis of Packed-Bed Latent Heat Thermal Storage System with Biomimetic Vein Hierarchical Structure, *International Journal of Green Energy*, 19 (2022), 6, pp. 592-602
- [6] Subramaniam, B. S. K., *et al.*, Performance Analysis of a Solar Dryer Integrated with Thermal Energy Storage using PCM- $\text{Al}_2\text{O}_3$  Nanofluids, *Environmental Science and Pollution Research*, 29 (2022), 33, pp. 50617-50631
- [7] Hu, Z., *et al.*, Study on Soil Heat Storage Performance and Operation Strategy of New Integrated HST-GSHO System in Different Cold Regions, *Energy and Buildings*, 854 (2022), Feb., 256
- [8] Lougou, B. G., *et al.*, Thermal and Electrical Performance Analysis of Induction Heating Based-Thermochemical Reactor for Heat Storage Integration into Power Systems, *International Journal of Energy Research*, 45 (2021), 12, pp. 17982-18001
- [9] Guan, Z., Cui, Y., Thermal Load Analysis and Control of Four-Stroke High Speed Diesel Engine, *Thermal Science*, 25 (2021), 4B, pp. 2871-2879
- [10] Yan, *et al.*, Study on the Performance of Double-Pipe Phase Heat Exchangers in Waste Heat Recovery with Heat Storage a Discharge, *Journal of Physics: Conference Series*, 2076 (2021), 1, 012002
- [11] Guo, B., Friction Heat Energy Recovery System Based on Hydraulic Brake System by Wire of Heavy Vehicle, *Thermal Science*, 27 (2023), 2A, pp. 1159-1166